Author(s): Immonen, Antti; Pettersson, Ante B. V.; Levikari, Saku; Peltonen, Heikki; Kyröläinen, Heikki; Silventoinen, Pertti; Kuisma, Mikko

Title: Thermal Measurement of Arterial Pulse using Heat Flux Sensors

Year: 2024

Version: Published version

Thermal Measurement of Arterial Pulse using Heat Flux Sensors

Antti Immonen, *Member, IEEE,* Ante B V Pettersson, Saku Levikari, *Member, IEEE,* Heikki Peltonen, Heikki Kyröläinen, Pertti Silventoinen, *Member, IEEE,* and Mikko Kuisma, *Member, IEEE*

***Abstract*— In this paper, the novel concept of using heat flux sensors (HFS) to measure arterial pulse on the skin surface is validated. The heat flux (HF) signal is compared with simultaneously measured electrocardiogram (ECG) and photoplethysmography (PPG) signals during both rest and initial recovery from exercise. It is found that the waveform measured with the HF sensor above the radial artery has similar shape to PPG and demonstrates a clear temporal alignment between the HF pulse waves and both the PPG and ECG signals. Further, it is shown that HF measurement can be used to consistently track the arterial pulse at varying skin-to-ambient temperature gradients.**

***Index Terms*— Blood Flow, Heat Flux Sensor, Plethysmography, Pulse Rate, Thermal Measurements, Wearable.**

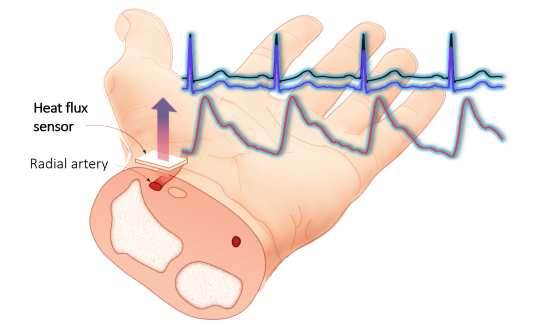

I. Introduction

CONTINUOUS and unobtrusive monitoring of vital parameters and health biomarkers through convenient, user-friendly wearable devices is of increasing interest in both wellness and healthcare settings. The cardiovascular system is commonly monitored via analysis of blood pulse waveforms collected using photoplethysmography (PPG).

In addition to the widely employed PPG measurements and the gold standard electrocardiogram (ECG), several methods have been developed for measurements of the cardiac rhythm. The arterial pulse has been measured by ballistographic methods [1], as well as by noncontact and remote photoplethysmography with infrared sensor elements in the ear [2] or thermal cameras [3], [4]. Thermal measurement of the arterial pulse can also be accomplished by employing a temperature sensor in contact with the skin, as reported in [5]. The present authors have also earlier demonstrated the use of a heat flux sensor (HFS) to measure arterial pulse [6].

Beyond simple measurement of heart rate, the arterial pulse waveform can be used to derive information on several systemic and local physiologic parameters. In the case of PPG, the demonstrated applications include blood pressure, cardiac output, stroke volume, vascular aging, and peripheral vascular disease, among others [7].

Recently, increased attention has been directed at the development of the thermal measurement capabilities of wearable devices, with a focus on skin temperature and noninvasive body core temperature measurements. Detailed solutions based on measured skin heat flux (HF) have been developed, e.g., for improved estimation of core temperature [8]–[10]. However, HF in itself has not yet been widely adopted in wearables as an indicator of the effects of blood flow or the thermoregulatory heat balance process. Measurement of the distribution and dissipation of heat based on observed thermal effects of blood flow could augment existing steady-state skin temperature measurements and better reveal the processes of thermoregulation. Improved measurement contextual awareness, e.g., recognition and measurement of the pulsatile heat component from arterial flow could provide a new viewpoint for the measurements.

In this study, we propose a method for skin-surface arterial pulse measurements using an HFS. We show that a waveform similar to a conventional PPG can be recorded, and that the timing and periodicity of the measured pulse waveform corresponds with both the optical plethysmogram and the electrocardiogram. In addition, the operating principle of the measurement is discussed based on observations on the measurements with two different HFS types.

This work was supported in part by the Academy of Finland (now the Research Council of Finland) under the project THERAD and in part by Business Finland under the project Q-Health. We would like to acknowledge the use of an ECG chest strap provided by VitalSignum Oy for the purpose of recording reference electrocardiogram signals in this study.

A. Immonen, S. Levikari, P. Silventoinen, and M. Kuisma are with the LUT School of Energy Systems, Lappeenranta–Lahti University of Technology, 53850 Lappeenranta, Finland (e-mail: firstname.surname@lut.fi.).

A.B.V. Pettersson is with the Department of Otorhinolaryngology-Head and Neck Surgery and the Department of Vascular Surgery, University of Helsinki and Helsinki University Hospital, Helsinki, Finland (e-mail: ante.pettersson@helsinki.fi).

H. Peltonen and H. Kyröläinen are with the Faculty of Sport and Health Sciences, Jyväskylä University, 40014 Jyväskylä, Finland (e-mail: firstname.surname@jyu.fi).

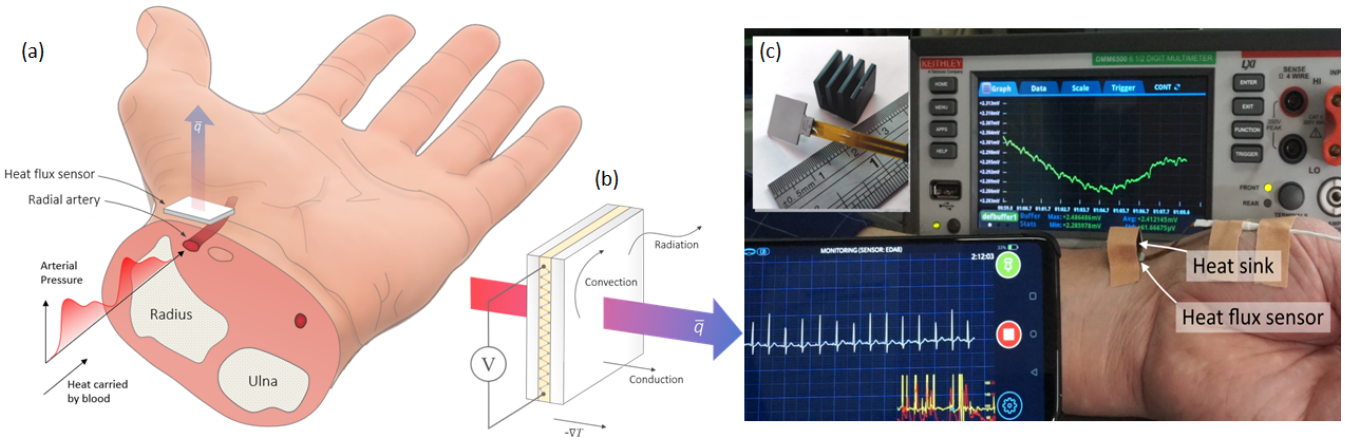

Fig. 1. Measurements. (a) Cross-sectional visualization of the proposed measurement on the wrist, where a pulsatile heat flux $\bar{q}$ originating from arterial blood flow is measured with a skin-surface-mounted heat flux sensor (HFS). The illustrated arterial pressure waveform is not to scale in the direction along the length of the blood vessel. (b) HFSs produce an output signal, typically a voltage signal, indicative of the heat flux $\bar{q}$ through the sensor based on a measured temperature difference across a transducer layer, shown in yellow. Heat may arrive at the surfaces of the sensor plate by means of conduction, convection, or radiation, or a combination thereof, but inside the sensor, heat coupling is limited to conduction. (c) Test with an HFS (GreenTEG gSKIN XP) attached directly to the skin and to the heat sink with a conductive adhesive. The sensor signal was recorded directly with a precision Digital Multimeter (DMM). Simultaneous measurements were made with a 1-lead Electrocardiogram (ECG) chest strap.

II. Methods

The human cardiovascular system works constantly to maintain a state of thermal balance in the body, carrying heat in accordance with the concurrent processes of metabolic heat generation and dissipation [11], [12]. The distribution of peripheral circulation is adjusted depending on the present thermal balance, resulting in, among other effects, changing magnitudes of blood flow to the extremities of the body caused by vasoconstriction and vasodilation [12].

When performing thermal measurements with skin-mounted wearable devices, the effects of thermoregulation can be difficult to isolate from those related to changing sensing conditions, such as mechanical skin contact, environmental temperature, or clothing [13]. Such uncertainties result in increased margins of error in applications based on measurement of body temperature and thermoregulation. Thus, increased knowledge about the measurement conditions is needed.

Because of the blood pulsation present in arteries, the heat dissipation from the body to the ambient experiences periodical changes, and right above the arteries these momentary changes in HF are accentuated enough to be measured on the skin surface by using a skin-surface-mounted HFS, Fig. 1a. The present measurement method is based on direct measurement of heat dissipated from skin to track the momentary thermal effects of the arterial pulse waveform.

The heat flux $\bar{q}$ describes the transfer of thermal energy, i.e., heat, by means of conduction, convection, or radiation [14]. In a one-dimensional setting, heat flux density by thermal conduction through a medium with the thermal conductivity k can be expressed by the temperature gradient ∇T according to Fourier's law [14] as

$$\bar{q} = -k\nabla T. \tag{1}$$

The operation of HFSs is typically based on monitoring the conduction of heat through the sensor. A well-characterized thermally conductive medium is combined with a transducer for measuring the temperature differential across the thickness of the sensor. Heat flux can then be inferred based on the measured temperature differential across the known thermal conductivity. The operation of a conventional HFS is illustrated in Fig. 1b.

The thermal resistance medium of the sensor can comprise, e.g., a thermopile circuit encased in a filler material. In such a case, the thermal resistance of the thermoelectric layer, in addition to the sensitivity of the thermoelectric transducer circuit, determines the output voltage signal of the sensor. Typical sensor implementations include mechanical support plates on the sides of the sensor that, while providing mechanical support, do not contribute to the output signal generation. In the case of transient heat flux measurements, such as the present measurement, the contribution of these support layers along with the thermal diffusivity of the sensing layer are the main determining factors affecting the response time of the sensor.

The proposed measurement focuses on the radial artery, where a characteristic pressure waveform is present, Fig. 2c. At the same time, a reference PPG measurement is performed on the skin surface. The PPG measurement inherently includes a signal originating from both the arterial flow and the proximate microvascular bed, which results in a different waveform, Fig. 2d. Similarly, the thermal waveform is expected to share characteristics of the sphygmogram and the plethysmogram.

A. Test setup

The feasibility of the proposed measurement method was evaluated on the wrist, with the heat flux sensor placed above the radial artery without using additional techniques to improve skin contact, such as abrasion or thermal interface gels. Two types of heat flux sensors were used: commercially available gSKIN sensors [1] (greenTEG, Switzerland) and a modified MEMS infrared sensor die (ZTP-135, Amphenol), as shown in Fig. 2. The study design comprised a sequence of

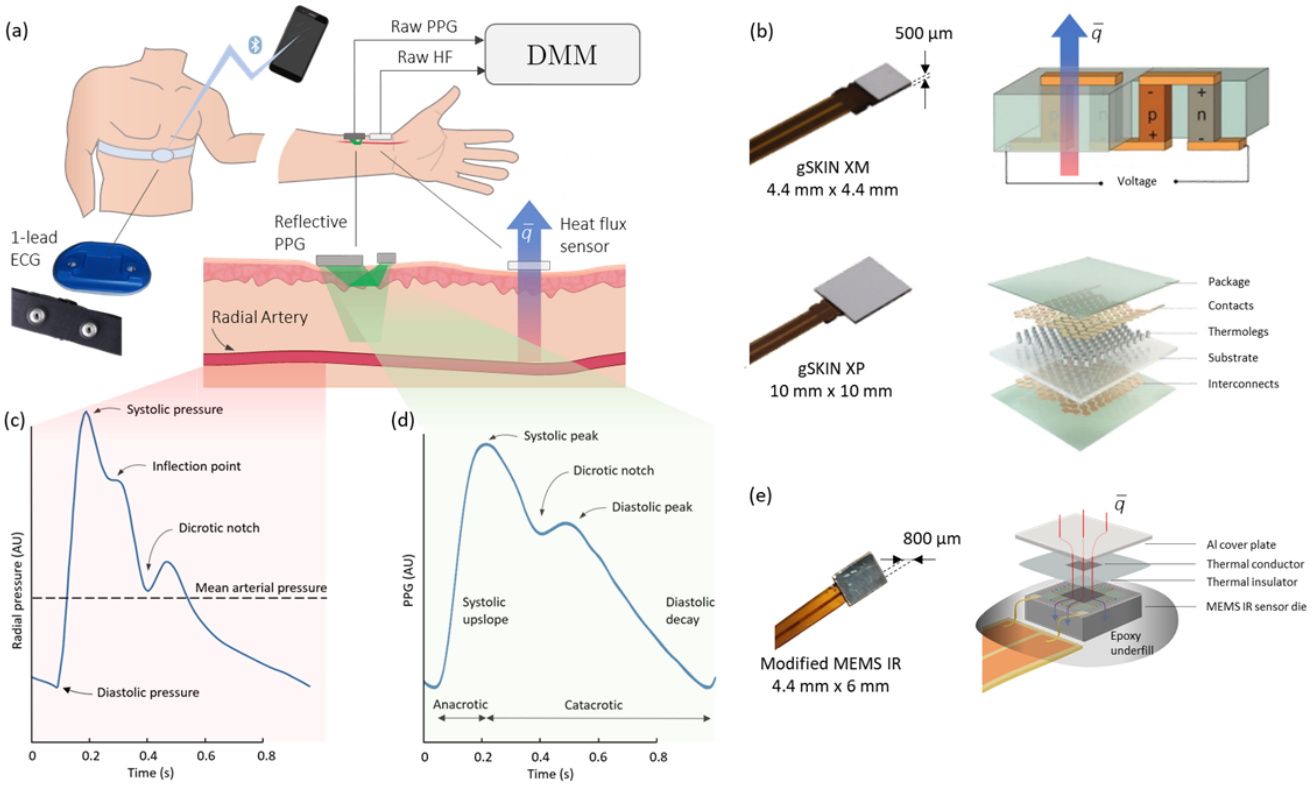

Fig. 2. Schematic illustration of the test setup and the sensors used in the measurements, along with typical arterial pressure and PPG waveforms. (a) Operating principles of the PPG and HF measurements on the skin. The raw signals of the PPG and the HF were recorded with a DMM, and the ECG was recorded using a mobile app. (b) Operating schematic of the commercial HF sensors used, modified from [15], [16], with the paths of the heat flow $\bar{q}$ shown. (e) Repackaged commercial MEMS infrared sensor die in a conductive heat flux sensing configuration, with $\bar{q}$ denoting the heat flow in both vertical and lateral directions inside the sensor. (c) Characteristics of the measured radial artery pressure waveform, adapted from [17], in comparison with the conventional PPG waveform (d), adapted from [18]. Typically, PPG signals primarily originate from the microvascular bed.

tests to investigate different aspects of signal transduction of the proposed method. Initial tests were performed to compare the waveforms of the photoplethysmography (PPG) and heat flux (HF) signals, as well as the temporal alignment of the peak in the pulse signal with the R wave in the ECG. Additionally, a test protocol with five subjects was designed to investigate the thermal signal waveform and amplitude under varying ambient temperatures.

The first measurements comprised initial concurrently acquired recordings of HF and PPG waveforms of three male test subjects aged 26 to 47 during rest in a seated position, with heart rates ranging from 65 bpm to 80 bpm. This test aimed to provide means to compare the waveforms of the optical and thermal waveforms, with the sensors placed side by side on the skin along radial artery. In this configuration, the timing of the pulse wave peaks was estimated to be similar enough for a fair comparison of the plethysmogram and the heat flux signal, Fig. 2. The thermal waveform recordings were made with a commercial greenTEG gSKIN XM heat flux sensor [15], while a conventional reflective PPG was recorded with a green light source. Both PPG and HF waveforms were recorded at a sampling frequency of 25 Hz. The initial tests were also utilized to investigate the shape of the heat flux waveform at different heart rates and the differences between the three different sensors of Fig. 2.

The second set of tests focused on measurement of the heat flux waveform in detail in different conditions. As an initial test, a set of measurements was made during first minutes of recovery from exercise. This test aimed to assess the consistency of the pulse measurement for the purposes of heart rate monitoring over several minutes in comparison with ECG-based heart rate measurement.

To examine how skin-to-ambient temperature difference affects the pulse signal obtained from a heat flux sensor, a test setup was designed with a heating and cooling Peltier element. Each subject had greenTEG gSKIN XP 10x10 mm heat flux sensor placed on their skin, with one side in direct contact with the skin on the top of the radial artery and the opposite side in contact with a copper block measuring 10x10x10 mm and weighing 8.936 g. The copper block temperature was varied above and below typical skin temperature to serve as a controlled heat source or sink. The temperatures of both the copper block and skin were measured with Pt100 sensors.

All signals in this setup were recorded with Dewesoft Sirius 8-channel data acquisition system with an STG amplifier module. The direct heat flux sensor signal was recorded at a sample rate of 500 Hz with an input range of 100 mV. The channel had a dynamic range of -137 dB, and an anti-aliasing filter with a corner frequency of 195 Hz was used.

Pulse waveform data was collected from five healthy male subjects aged 30-58. The measurements were conducted in a controlled environment where the ambient temperature was

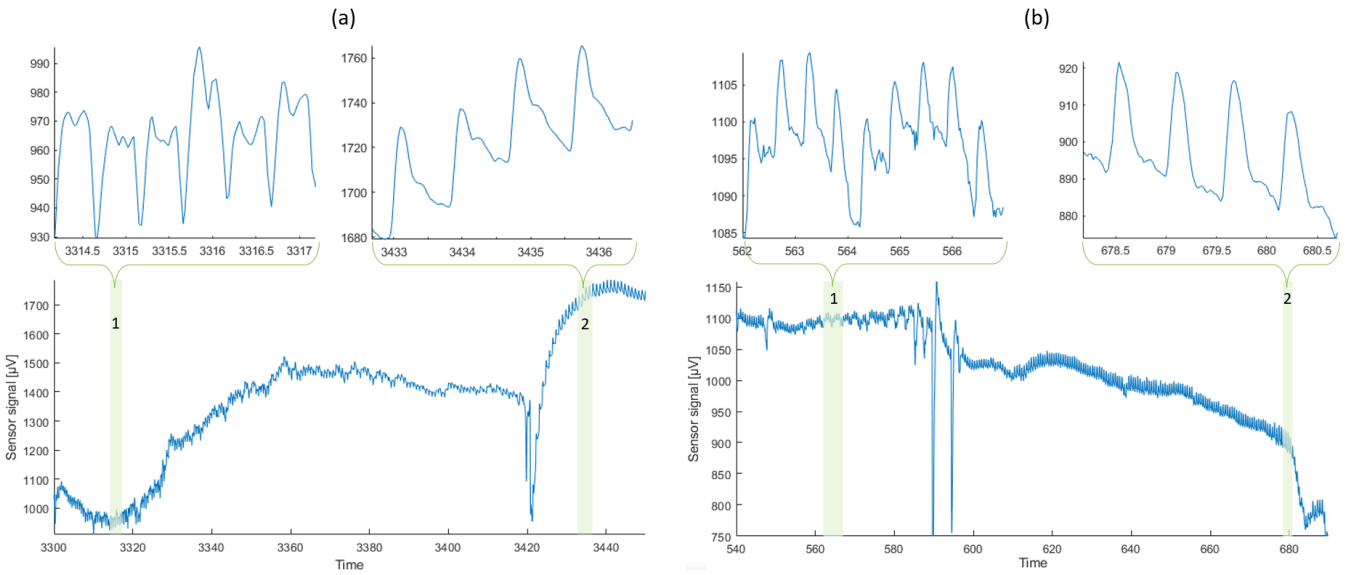

Fig. 3. 150 s long example signals of different measurements show changes in the measured waveforms as influenced by sensor sensitivities and response times. Details of the waveforms are highlighted, showing changing pulse amplitudes, DC baseline levels, and pulse waveforms for the different sensor types and measurement contexts. The pulse amplitudes of the displayed waveforms span from 15 µV to 40 µV for gSKIN (a) and from 10 µV to 30 µV for the MEMS sensors (b), respectively. In (a), an observable difference in the gSKIN sensor waveform characteristics coincides with the local heat flux minima (1) and maxima (2). In (b), the high movement artifact susceptibility of the measurement is exemplified by breathing-related artifacts (1).

artificially manipulated to create different temperature gradients. The hand of the subject, with the sensors attached to the wrist, rested on a table and was covered with a cardboard box to minimize movement and airflow artifacts during the measurement. Five-minute resting (sitting) measurements were conducted using an HFS, two Pt100 sensors, and an ECG reference. The ECG signal was recorded using a Vital Signum chest strap electrode connected directly to the Dewesoft data acquisition system.

From the longer (5-6 min) measurement series, segments with sufficiently artifact-free signal were manually selected based on visual inspection of the time series. From each segment, five consecutive pulses were extracted and averaged to obtain the presented mean pulse peak-to-peak voltage and temperature values. The averaging was synchronized with the ECG reference signal. The moving average of a single pulse was calculated over a 0.7-second interval, corresponding to a heart rate of approximately 85 bpm.

III. Results

A. Heat flux pulse waveform

Initial measurements were made in variable configurations to reveal aspects of signal transduction in different configurations. Two different HF sensors (gSKIN XM and MEMS prototype) were used to investigate signal amplitudes and response times at varying heart rates. Fig. 3 presents one-minute excerpts of the acquired raw data during the measurements, showing a typical sensor output.

Like in the case of a PPG, a signal comprising of both a slowly changing DC component and a weak pulsatile AC component was observed. Both sensor types in these initial tests exhibited relatively weak signals, with the sensitivities of the HFSs being barely sufficient to record the pulse waveforms. Typical DC levels ranged between 1.5 mV to 5 mV and from 0.5 mV to 1.5 mV for the gSKIN and MEMS sensors, respectively, while the pulsatile AC components had nearly an order of magnitude lower amplitudes. The measured AC signals ranged from 1 µV to 45 µV for the gSKIN and 10 µV to 25 µV for the MEMS sensor. For the calibrated gSKIN XP sensor with a sensitivity of approximately 20 µV/(W/m^2) [15], a peak-to-peak pulsatile amplitude of 40 µV (Fig. 3) corresponded to a heat flux of around 2 W/m^2.

Next, a comparison was made between PPG and HF waveforms. To improve the quality of the signal, averaged waveforms of 20 consecutive pulse waves were calculated for both signals. Fig. 4d illustrates the similarities and differences between the HF and PPG waveforms for one subject at the HR of 79 BPM. The measured PPG waveform displayed the characteristic plethysmographic shape described in the literature (Fig. 2c), with significant variability in the exact waveform depending on sensor contact pressure and the exact sensor location.

Next, the measurements were repeated at elevated heart rates using only the MEMS sensor, investigating the consistency of the pulse waveform acquisition. The observed signal amplitude varied with heart rate, the peak-to-peak amplitude being 16 µV at 67 BPM, 25 µV at 96 BPM, and 10 µV at 156 BPM, with the noise levels ranging from approximately 1 µV to 2 µV in all cases. The observations were again averaged from 15 consecutive pulse waves for each case, using a 0.72 s window length, Fig. 4b.

These measurements confirmed that across different sensor types and heart rates ranging from 69 BPM to 156 BPM, the recorded arterial pulse waveform closely resembled a

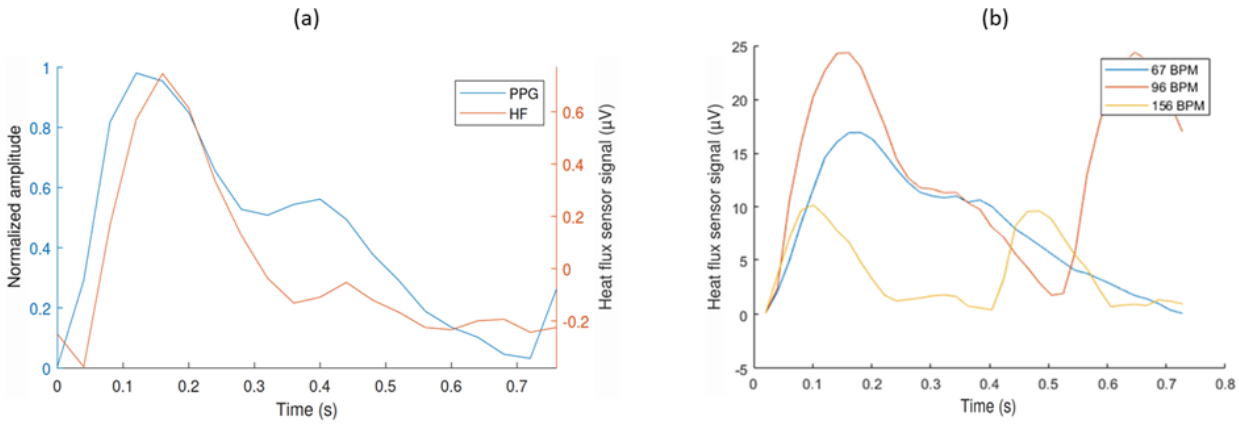

Fig. 4. Pulse waveforms of the studied heat flux and PPG sensors. (a) Concurrently recorded averaged waveforms (20 consecutive pulses) of both green light PPG and HF show similar plethysmographic characteristics between the optical and thermal signals at a resting HR of 79 BPM. (b) Comparison of the pulse waveforms at a resting HR of 69 BPM, along with postexercise HRs of 156 BPM and 96 BPM validates the concept of thermal HR measurement at higher HR values. All waveforms are averages of 15 pulse waves with a window length of 0.72 s.

conventional PPG waveform and the radial artery pressure waveform [1].

These initial measurements demonstrated that when positioned above the radial artery, a skin-surface heat flux measurement exhibited waveform characteristics closely tracking arterial pulse waves. These tests provided practical examples of heat flux measurements with a fast enough response to accurately record arterial pulse waveforms, even at higher heart rates (Fig. 4b).

B. Heat flux waveform and HR detection in comparison with ECG

The timing of the HF signal was compared with the ECG. Initially, the alignment of the HF signal and the ECG signal was performed to examine their temporal correspondence. Fig. 5 depicts the waveform of the HFS and the ECG measurement for the selected eight-second period.

The peak positions of the signal produced by the HFS show a relative temporal alignment with the ECG signal and the corresponding momentary variations. A comparison of the time series data validates that the signal recorded with the HF sensor corresponds with the HR calculated from ECG.

Next, postexercise measurements were conducted for several minutes. A time-frequency analysis, a spectrogram, was used to monitor the change in heart rate during recovery after exercise, Fig. 6.

With a spectrogram, the temporal variation in the frequency content of the signal can be represented graphically in the time–frequency domain. The spectrogram has also been used in classification of cardiac arrhythmias [19], [20].

Spectrograms of both the heat flux measurement and the reference ECG measurement of the 4 min test are shown in Fig. 6. Both the ECG and HF signals display a similar decrease in HR, dropping from approximately 140 BPM to below 100 BPM. Notably, a subject in this study experienced cardiac arrhythmias during one of the tests. While this occurrence was unplanned, we have intentionally selected this data in Fig. 6 to demonstrate the temporal correspondence between the HF signal and the ECG during abnormal cardiac activity.

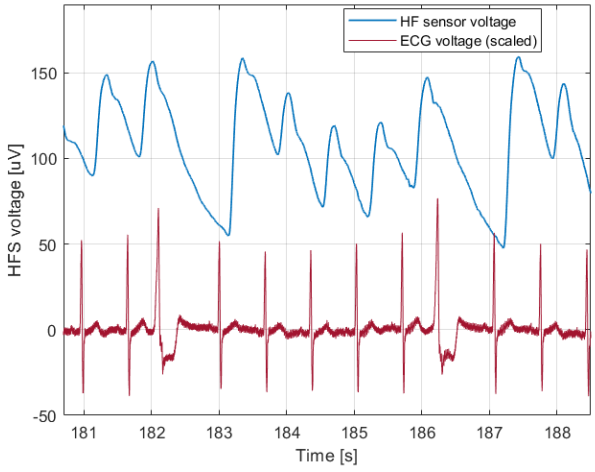

Fig. 5. Example of matching waveforms of unfiltered heat flux (blue) and ECG signals. Signals are temporally aligned, and momentary changes of heart rate can be seen in both signals. Two premature heart beats (extrasystoles) are shown in the ECG (t = 182 and t = 186), and after these arrhythmias no HF pulse signal is detected. These arrhythmias are shown as vertical lines in spectrograms, Fig. 6.

The distinct peaks, A–G in Fig. 6, are visible in both spectrograms and are temporally synchronized, although the SNR in the heat flux signal is lower and the features are not as clear as in the ECG. Overall, the HF signal temporally corresponds with ECG, showing a similar response to the changing heart rate and temporal variations. This confirms that both the separate measurement methods measure HR, and that the measured HF waveform is indicative of the arterial pulse. This test also demonstrates that the HF signal can be used to track pulse rates for longer period of time. Beyond these demonstrations, no further analysis was carried out on any data with distinct episodes of arrythmia.

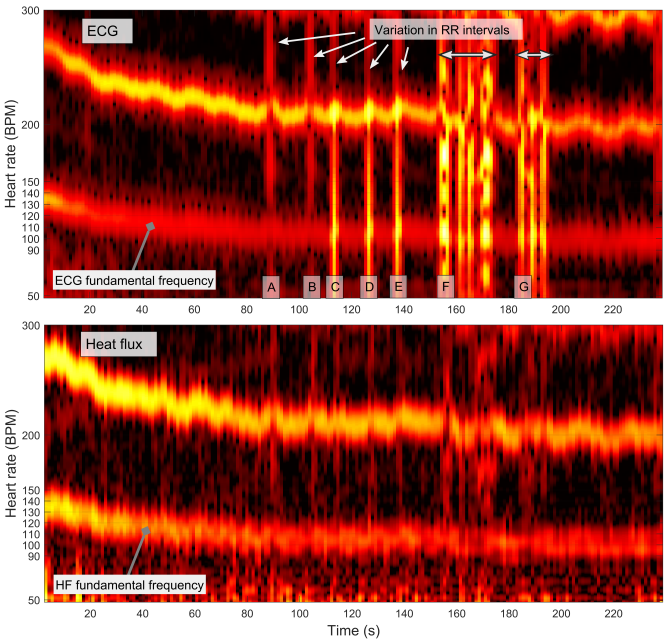

Fig. 6. Spectrograms of unfiltered heat flux and ECG signals display a temporal match. Postexercise signals also show a declining heart rate during 4 min, when the fundamental frequency decreases from approximately 140 to 100 BPM. Momentary changes in heart rate and instances of cardiac arrhythmia appear as a broad frequency content, and thus, as vertical lines in the image between 80 and 200 s. Peaks A–G are visible in both spectrograms and are temporally synchronized.

C. Ambient temperature effects on pulse signal transduction

The final test demonstrated the significant influence of skin-to-ambient temperature gradient on pulse signal amplitude.

A scatter plot, Fig. 7, shows the measured peak-to-peak voltage of the arterial pulse signal measured with an HFS, including 57 separate measurement points. The horizontal axis represents the temperature difference between the skin and the ambient environment, positive value indicating that the skin temperature is higher than the ambient temperature. The vertical axis represents the peak-to-peak voltages of the measured HF signals.

This scatter plot shows the impact of skin-to-ambient temperature difference on the pulse signal of the HFSs: larger differences (both positive and negative) resulted in stronger HF pulse readings, while smaller differences produced weaker signals. However, the dependence on temperature difference is nonlinear, with a pulse still present at zero temperature difference.

The histogram in Fig. 8, reveals a skewed distribution of the measured peak-to-peak voltage. This was modeled as a Rayleigh distribution with a mode of 41.3 µV (most frequent value) and a scale parameter σ of 7.6.

Our findings demonstrate that changes in skin-to-ambient temperature affect the HF and pulse signal measured by the sensor. However, this dependence is not linear, with a pulse still detectable even at zero temperature difference. Importantly, the sensor's pulse response is also influenced by factors beyond temperature, such as sensor location, variations in skin thermal conductivity, and subject movement artifacts.

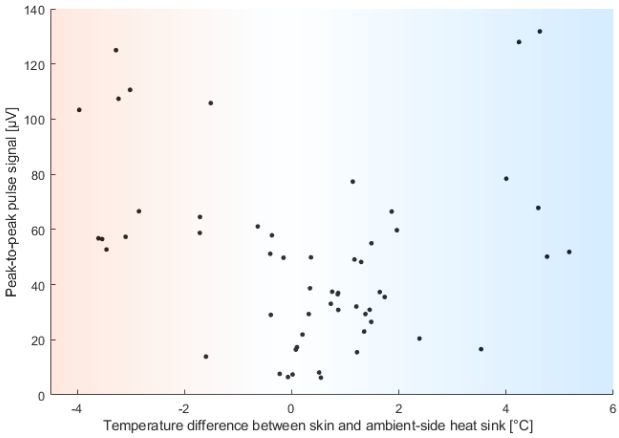

Fig. 7. Scatter plot of the observed relationship between the acquired peak-to-peak pulsatile sensor signal and the skin-to-ambient temperature difference. A positive temperature difference means that the skin temperature is higher than the ambient temperature, and vise versa. Additionally, an approximate subject-perceived heat sink temperature is illustrated as a color gradient spanning from thermoneutral (white) to warm (orange) and cool (blue) sensations. Pulse signals were successfully acquired in all conditions, with notably increased amplitudes in both heated and cooled heat sink conditions.

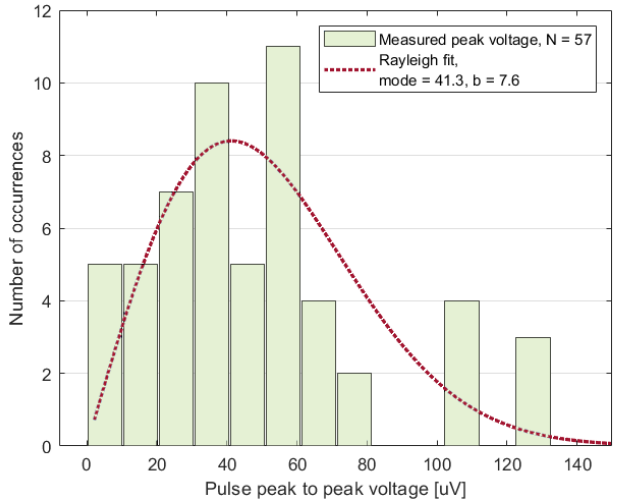

Fig. 8. Histogram of the acquired peak-to-peak heat flux pulse signal. The distribution exhibits a positive skew, indicating a higher frequency of lower voltage values. The mode, representing the most frequent voltage, is 41.3 µV.

These factors were not explored in this study. Limitations of the test setup include a small sample size and a controlled environment with an emulated ambient temperature.

IV. Discussion

The presented measurements prove the applicability of the proposed method across different ambient temperatures, heart rates and sensor types. The signals, while often weak in amplitude could be consistently tracked. In the final test protocol it was shown that the measurement capability is not limited by the DC HF level of the measurement. When the ambient side of the sensor was hotter than the skin, the waveform of the pulsatile component was observed to be inverted. Even at a measured average DC level of 0 W/m^2, i.e., temperature differential of 0°C, the sensor could still record a measurable

TABLE I
SENSOR AND SIGNAL CHARACTERISTICS OVERVIEW

Parameter	Skin heat flux	gSKIN XP	fSKIN XM	MEMS sensor
Pulsatile signal	0.1 to 4.5 W/m^2	3 µV to 130 µV	1 µV to 30 µV	7 µV to 35 µV
Typical DC Level	100-500 W/m^2	1 mV to 19 mV	1 mV to 2 mV	0.2 mV to 1.5 mV
Noise level	-	200 nV p-p	200 nV p-p	1 µV p-p
Maximum skin contact artifact	-	70 mV	27 mV	4 mV
DC Baseline settling time (90%)	-	10 s	10 s	5 s

pulse signal. This is possible because the average DC level can remain at close to 0 W/m^2 while heat is being exchanged back and forth between the skin or the thermal mass of the heat sink is very large compared to the amount of heat transferred during a pulse.

The findings of this work bring limited insight into the thermal coupling mechanisms of the measured heat flow from the radial artery. On one hand, the thermal effects may result from changes in heat conduction in the tissue between the artery and the sensor. On the other hand, pulsatile mechanical movement might simply modulate the thermal contact of the sensor and the skin like in the case of a sphygmogram. The latter seems likely to be the dominant effect, when considering the thermal properties of the system.

The thermal system can be better understood through a holistic view, spanning from the subject to the measurement device. To this end, a lumped element T-ladder thermal equivalent circuit (Fig. 9) was formed to elucidate the main thermal characteristics and the ensuing technical requirements for measurement. In the model, the pulsatile component of blood flow is an AC thermal current source, from where the heat current then propagates into a thermally volume-conducting medium, i.e., the subcutaneous tissues, dermis, and epidermis. These intermediary components can be thought as a continued-fraction T-ladder circuit of thermal resistances and thermal capacitances, where an increased distance between the artery and the measurement point result in a reduced measured signal amplitude. The properties of the first part of the model, shown on the left side in Fig. 9, are dependent on the physiological parameters such as skin thermal resistance properties and possibly on the applied contact pressure.

The second part of the thermal equivalent circuit is comprised of the sensor and any additional measurement instrumentation present. Here, the sensor acts as a thermal conductor, through which the measured pulsatile heat is transferred to a heat sink, and finally dissipated to the environment. In order to not limit the bandwidth of the measurement, the sensor surface layers and the sensing layer should not have limiting thermal time constants, i.e. excess thermal mass.

Table I shows an overview of the measured heat signal and the performance of the sensors that was sufficient to record the signals. In order to make the measurements feasible, based on the present results, the sensors should have a sensitivity of at least 1 µV/(W/m^2) or better, and a response time of under 50 ms. Additionally, the sensor assembly should, on the cold side, include some form of a heat sink that is large enough to not warm up during individual pulses to maintain a temperature difference across the sensing layer. Further, the results showed that an added thermal capacity of a heat sink on the cold side of the sensor stabilized the DC behavior of the system, and provided a slightly increased signal amplitude by increasing the temperature difference across the sensor.

Assuming an average thermal diffusivity of $\alpha = 0.1$ mm^2/s of the tissue separating the radial artery and the sensor based on the table of [21] and a minimum arterial distance of L = 0.5 mm from the sensor when pressed firmly, the thermal wave timescale is roughly $t = L^2/\alpha = 2.5$ s at the lowest. Similar thermal wave propagation times can also be gathered from [22]. The estimated time constant suggests that majority of the thermal pulse conducted from the artery is attenuated inside the thermally volume-conducting tissue on the way to the skin and the sensor, and that the measured periodicity in HF thus probably originates from tissue closer to the sensor.

Despite uncertainties around the exact coupling mechanism, the proposed method can be used to monitor the thermal effects of blood flow with high enough precision for the arterial pressure waveform to be visible, even at higher heart rates. In addition to providing a new way to record the pulse waveform, the measurement can reveal processes related to the thermal effects of blood flow on the tissue surrounding the artery, both at the timescale of one pulse as well as longer term effects.

Measurement of heat flux with the context of arterial location can provide information beyond just the arterial pulse waveform. The thermal waveform specifically related to the arterial flow HF waveform could be a basis of new kind of noninvasive analyses. Information derived within the arterial region heat transfer context could possibly be utilized as a noninvasive systemic biomarker, offering insights into thermoregulation, blood flow, and metabolic heat production. Further, the HF signal could be used to detect the localized thermal effects of the blood flow on the tissue under the sensor, where the volumetric flow of blood exchanges heat with the tissue. The rate of this heat exchange under the skin then modulates the HF and its distribution on the skin surface. This information, in turn, could then be utilized for analyzing the amount of peripheral blood flow, tissue perfusion, and vasomotor responses of thermoregulation. Thus, increased understanding of the thermal signature of the arterial area temperature and heat distribution could improve the estimation of arterial blood temperature or overall peripheral dissipation of metabolic heat.

The combination of the thermal effects of blood flow and access to the thermal pulse waveform could be a basis for several new applications. For example, the information could be used to precisely locate a thermal reference point above an artery on the skin, or to provide a relative reference on the rate of heat transfer by blood flow.

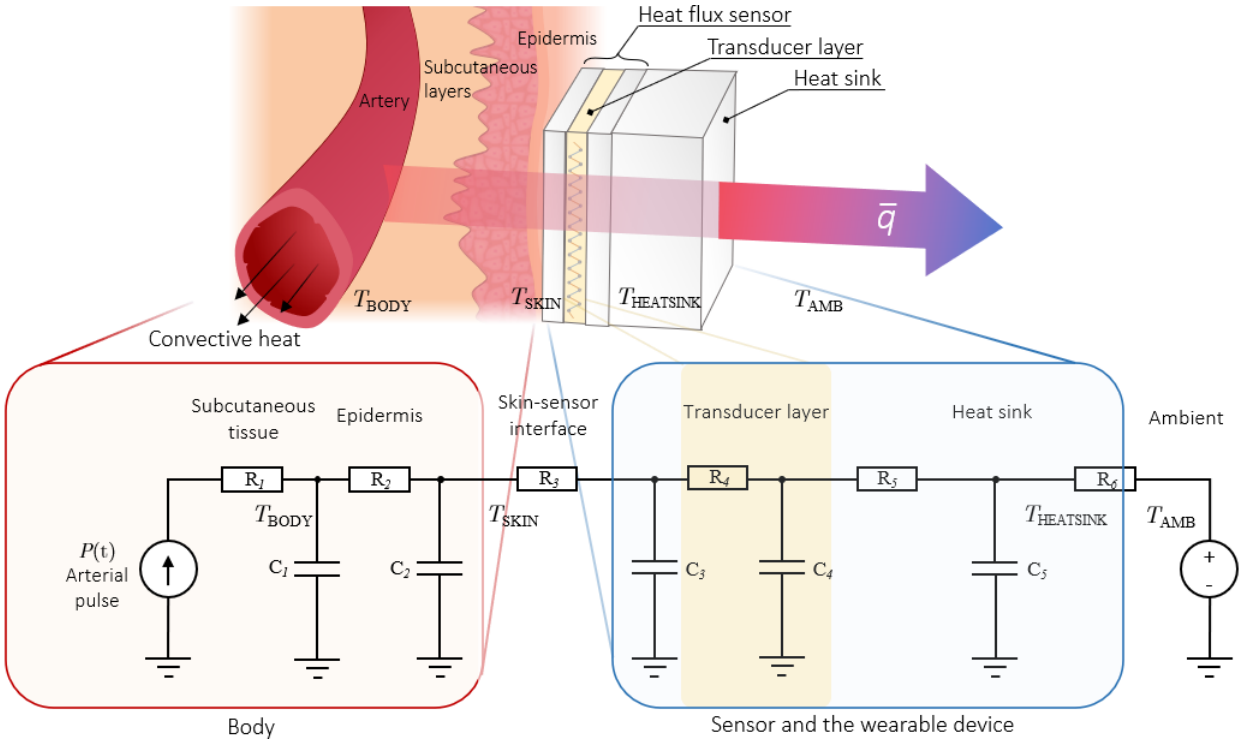

Fig. 9. Behavior of the time-dependent thermal field in which the measurement takes place can be simplified into a lumped thermal equivalent circuit model. The pulsatile component of the heat carried by blood is dampened by the present subcutaneous tissues and the skin–sensor interface. The signal of interest is transduced in the region shown in yellow, its magnitude depending on both the sensitivity and response time of the sensor. Numerous properties of the sensor and the mechanics of the wearable device can also play a significant role in the formation of the eventual output signal.

V. Conclusion

A novel pulse measurement method based on HF measurement was validated against conventional PPG and ECG methods. The results showed that an HFS placed on the skin surface can be used for recording the radial artery pulse waveform. The recorded waveform shared features with the PPG, and had a similar peak-to-peak timing to the ECG. The measurements were repeated at different heart rates and with different practical heat flux sensor designs.

The pulsatile heat flux signal had similarities in temporal characteristics when compared with the PPG and ECG reference signals, and thus, it may also allow the use of a pulse shape for a more detailed analysis of cardiac function.

Direct measurement of the time-dependent thermal effects of blood flow can enable new methods for and applications in wearable estimation of the thermoregulative functions. The proposed measurement could be used as a new source of arterial pulse information, e.g., on wrist-worn devices, and to improve wearable thermal measurements.

References

[1] M. Kaisti, T. Panula, J. Leppänen, R. Punkkinen, M. J. Tadi, T. Vasankari, S. Jaakkola, T. Kiviniemi, J. Airaksinen, P. Kostiainen *et al.*, "Clinical assessment of a non-invasive wearable MEMS pressure sensor array for monitoring of arterial pulse waveform, heart rate and detection of atrial fibrillation," *NPJ digital medicine*, vol. 2, no. 1, pp. 1–10, 2019.

[2] G. de Graaf, D. K. Cruz, J. C. Haartsen, F. Hooijschuur, and P. J. French, "Heart rate extraction in a headphone using infrared thermometry," *IEEE Transactions on Biomedical Circuits and Systems*, vol. 13, no. 5, pp. 1052–1062, 2019.

[3] S. Zaunseder, A. Trumpp, D. Wedekind, and H. Malberg, "Cardiovascular assessment by imaging photoplethysmography–a review," *Biomedical Engineering/Biomedizinische Technik*, vol. 63, no. 5, pp. 617–634, 2018.

[4] X. Chen, J. Cheng, R. Song, Y. Liu, R. Ward, and Z. J. Wang, "Video-based heart rate measurement: Recent advances and future prospects," *IEEE Transactions on Instrumentation and Measurement*, vol. 68, no. 10, pp. 3600–3615, 2018.

[5] A. Cuadras and O. Casas, "Determination of heart rate using a high-resolution temperature measurement," *IEEE Sensors Journal*, vol. 6, no. 3, pp. 836–843, June 2006.

[6] A. Immonen, S. Levikari, H. Peltonen, M. Silvennoinen, H. Kyröläinen, A. V. Mityakov, P. Silventoinen, and M. Kuisma, "Measuring heart rate with a heat flux sensor," in *2021 IEEE International Instrumentation and Measurement Technology Conference (I2MTC)*, 2021, pp. 1–6.

[7] J. Park, H. S. Seok, S.-S. Kim, and H. Shin, "Photoplethysmogram analysis and applications: An integrative review," *Frontiers in Physiology*, vol. 12, 2022.

[8] X. Ren, C. Zhou, and X. Ye, "A novel miniaturized sandwich-like sensor for continuous measurement of core body temperature," *IEEE Sensors Journal*, vol. 22, no. 17, pp. 16 742–16 749, 2021.

[9] A. Conway, M. Bittner, D. Phan, K. Chang, N. Kamboj, E. Tipton, and M. Parotto, "Accuracy and precision of zero-heat-flux temperature measurements with the 3m™ bair hugger™ temperature monitoring system: a systematic review and meta-analysis," *Journal of Clinical Monitoring and Computing*, vol. 35, no. 1, pp. 39–49, 2021.

[10] N. Verdel, T. Podlogar, U. Ciuha, H.-C. Holmberg, T. Debevec, and M. Supej, "Reliability and validity of the core sensor to assess core body temperature during cycling exercise," *Sensors*, vol. 21, no. 17, p. 5932, 2021.

[11] A. A. Romanovsky, "The thermoregulation system and how it works," *Handbook of clinical neurology*, vol. 156, pp. 3–43, 2018.

[12] C. L. Lim, "Fundamental concepts of human thermoregulation and adaptation to heat: a review in the context of global warming," *International Journal of Environmental Research and Public Health*, vol. 17, no. 21, p. 7795, 2020.

[13] B. A. MacRae, S. Annaheim, C. M. Spengler, and R. M. Rossi, "Skin temperature measurement using contact thermometry: a systematic

review of setup variables and their effects on measured values," *Frontiers in physiology*, vol. 9, p. 29, 2018.
[14] P. Childs, J. Greenwood, and C. Long, "Heat flux measurement techniques," *Proceedings of the Institution of Mechanical Engineers, Part C: Journal of Mechanical Engineering Science*, vol. 213, no. 7, pp. 655–677, 1999.
[15] GreenTEG, *Heat flux sensor gSKIN® series datasheet*, 2020, retrieved March 9, 2020. [Online]. Available: https://shop.greenteg.com/heat-flux-measurement-heat-flux-sensor-gskin-xm/
[16] S. K. Singh, M. K. Yadav, and S. Khandekar, "Measurement issues associated with surface mounting of thermopile heat flux sensors," *Applied Thermal Engineering*, vol. 114, pp. 1105–1113, 2017.
[17] M. F. O'Rourke and J. B. Seward, "Central arterial pressure and arterial pressure pulse: new views entering the second century after korotkov," in *Mayo Clinic Proceedings*, vol. 81, no. 8. Elsevier, 2006, pp. 1057–1068.
[18] P. H. Charlton, P. A. Kyriacou, J. Mant, V. Marozas, P. Chowienczyk, and J. Alastruey, "Wearable photoplethysmography for cardiovascular monitoring," *Proceedings of the IEEE*, vol. 110, no. 3, pp. 355–381, 2022.
[19] M. Salem, S. Taheri, and J.-S. Yuan, "Ecg arrhythmia classification using transfer learning from 2-dimensional deep cnn features," in *2018 IEEE biomedical circuits and systems conference (BioCAS)*. IEEE, 2018, pp. 1–4.
[20] A. M. Alqudah, S. Qazan, L. Al-Ebbini, H. Alquran, and I. A. Qasmieh, "Ecg heartbeat arrhythmias classification: a comparison study between different types of spectrum representation and convolutional neural networks architectures," *Journal of Ambient Intelligence and Humanized Computing*, vol. 13, no. 10, pp. 4877–4907, 2022.
[21] K. Giering, O. Minet, I. Lamprecht, and G. Müller, "Review of thermal properties of biological tissues," pp. 45–65, 1995.
[22] A. Sagaidachnyi, A. V. Skripal, A. Fomin, and D. Usanov, "Determination of the amplitude and phase relationships between oscillations in skin temperature and photoplethysmography-measured blood flow in fingertips," *Physiological measurement*, vol. 35, no. 2, p. 153, 2014.

Antti Immonen was born in 1993 in Finland. He received the B.Sc. and M.Sc. degrees from LUT University, Lappeenranta, Finland, in 2018 and 2019, respectively.

He is currently a Doctoral Student with LUT Laboratory of Applied Electronics. His main research topics include thermoelectric devices, sensors and biophysical instrumentation.

Ante Pettersson was born in 1983 in Finland. He received his Doctor of Medicine from Helsinki University in 2010. He has since studied mechanical engineering at Lappeenranta University of Technology (LUT) and worked as a research fellow at the Peter Gilgan Center for Research and Learning at the Hospital for Sick Children in Toronto, Canada. Currently a resident of Vascular Surgery at Helsinki University Central Hospital and a doctoral student at Helsinki University, his research interests include medical 3D-printing, bioprinting and omics technologies.

Saku Levikari was born in 1991 in Finland. He received the B.Sc. and M.Sc. degrees from Lappeenranta University of Technology (LUT), Finland, in May and June of 2018, respectively. He is currently a doctoral student with LUT School of Energy Systems, Laboratory of Applied Electronics. His research interests are in the field of data analytics and machine learning, with topics ranging from biosignal measurements to power electronics reliability.

Heikki Peltonen received his PhD in Biomechanics from the University of Jyväskylä, Finland with a topic: Isometric force-time parameters in monitoring of strength training – with special reference to acute responses to different loading resistances. He is currently working as a postdoctoral researcher in the Faculty of Sport and Health Sciences, University of Jyväskylä. Furthermore, he is the member of the advisory board of the NeuroMuscular Research Center. His research interests include health monitoring, acute neuromuscular responses, and long-term adaptations to different types of exercise training. He has several years of experience in the development process of performance monitors and healthcare solutions.

Heikki Kyröläinen, PhD, FACSM, is a Professor in the Faculty of Sport and Health Sciences, University of Jyväskylä, Finland. He was found competent for professorships in Exercise Physiology in 2003, Biology of Physical Activity in 2005, Kinesiology in 2006, and Biomechanics in 2007. He has published over 180 peer-reviewed international scientific papers and about 300 chapters in books, abstracts, proceedings, and domestic publications. His research interests are wide in the field of biology of physical activity but, however, a major research line has been mechanical efficiency and economy during human locomotion since 1987.

Pertti Silventoinen was born in Simpele, Finland, in 1965. He received the DSc degree from Lappeenranta University of Technology (LUT), Lappeenranta, Finland, in 2001. He became a professor of applied electronics in 2004. His current research interests include power electronics systems in various applications.

Mikko Kuisma was born in Finland, in 1971. He received the M.Sc. degree in electrical engineering and control systems and the D.Sc. degree in electronics from Lappeenranta University of Technology (LUT), Finland, in 1997 and 2004, respectively. He became an Associate Professor of Applied Electronics in 2002. Since 1995, he has been working in the field of electronics, sensors, acoustics, IoT, EMC, and engineering education. His current research interests include measurement electronics and sensors in various applications.